

In-medium properties of Θ^+ in symmetric nuclear matter*

X. H. Zhong[†] P. Z. Ning[‡]

Department of Physics, Nankai University, Tianjin 300071, P. R. China

December 2, 2024

Abstract

The properties of nuclear matter is carefully analysed in relativistic mean-field formalism(RMF), it is found that the non-linear self-interaction of σ meson affects the properties strongly at high density and there is also strong parameter dependence in this region. We introduce a density dependent scalar coupling according to the idea of QMC model, find that its effect to properties of nuclear matter is little at low density, however, the effect at high density is obviously. The Θ^+ (as an structureless particle) effective masses in medium is studied, $M_{\Theta^+}^* \simeq 0.67M_{\Theta^+}=1030$ MeV at normal nuclear density. The density dependent scalar coupling obviously affects the baryon effective masses in nuclear matter, especially at high density. We review the kaon meson in medium and find the RMF model considered density dependent coupling is consistent with ChPT model in a certain extent. We develop another method to describe the Θ^+ in RMF, find the effective mass $M_{\Theta^+}^* \simeq 0.73M_{\Theta^+}=1120$ MeV much larger than the usual RMF prediction; the potential depth of Θ^+ in nuclear matter with the new method is $U_{\Theta^+} \simeq -37.5$ MeV much shallower than $U_{\Theta^+} \simeq -90$ MeV predicted with the usual RMF.

PACS: 21.65+f, 21.30.Fe

Key words: relativistic mean field, nuclear matter, Θ^+ , effective mass

1 Introduction

The study of in-medium properties of hadrons is a topic of interest^[1-4]. Relativistic heavy-ion collisions of nuclei opens the possibility of investigating hadrons in hot and dense hadronic matter, which makes the topic become more attractive. The importance of in-medium properties of hadrons is that the changes in nuclear medium could be a signal of the formation of hot hadronic and /or quark-gluon matter. There are several theoretical efforts made to understand the behavior of hadrons in dense matter, such as QCD sum rules^[4], quark-meson coupling model^[1] and relativistic mean field approach^[31].

*Supported by National Natural Science Foundation of China (10275037) and Specialized Research Fund for the Doctoral Program of Higher Education of China (20010055012)

[†]E-mail: zhongxianhui@mail.nankai.edu.cn

[‡]E-mail: ningpz@nankai.edu.cn

Relativistic mean field is a convenient method for us to study nuclear many body problems. It has been widely used to predict the properties of nuclear matter and finite nuclei. Not only ordinary but also hyper-nuclei/ nuclear matter are described well in RMF^[5–12]. One of the important aspects for RMF is how to determined the effective interactions of meson-baryon couplings. To describe the nuclear matter and finite nuclei well, the nonlinear self-interactions for σ meson and/or ω meson are introduced^[13, 14]. In recent years, a number of effective interactions of meson-baryon couplings such as NL-Z^[5], NL3^[6], NL-SH^[15], TM1 and TM2^[16] are developed. However, all the sets have their limit in predicting the properties of nuclear matter or finite nuclei and the constant couplings may be not practical at high density. In the present paper, we will study how much the nonlinear self-interactions for σ meson affect the properties of nuclear matter and how much there is parameter dependence. Considering the effect of nuclear density on the coupling constant, we try to introduce a density dependent scalar coupling in RMF.

The study of properties of nuclear matter in RMF makes us conveniently investigate the in-medium properties of the new discovered baryon Θ^+ . The pentaquark state Θ^+ (1540) with strangeness +1, first predicted by Diakonov *et al.*^[17], has been nearly confirmed^[18–24]. It has been listed by the Particle Data Group in the review of particle physics^[25]. Therefore, it is natural to study the properties of Θ^+ in nuclear medium with positive strangeness. In fact, the Θ^+ in nuclear medium has attracted many groups' interesting^[26–30]. Since Miller predicted there is an attractive Θ -nucleon interaction strong enough to bind Θ^+ in nucleus^[26], D. Cabrera et al. found a large attractive Θ^+ potential 60 \sim 120 MeV in the nuclear medium associated to the two meson cloud of the antidecuplet^[28]. In our previous work^[12], we studied Θ^+ hypernuclei in RMF, predicted the attractive Θ^+ potential is 50 \sim 90 MeV. And in the other prediction such as QCD sum-rules gives an attractive Θ^+ potential 40 \sim 90 MeV^[29] and quark mean-field model provides an attractive Θ^+ potential of \sim 50 MeV^[30]. Although all the models predict an attractive Θ^+ potential, the potential depth is still far from accurate predicted. In this work we will study Θ^+ potential depth in nuclear matter in RMF with a new approach. In this approach, we consider the structure of Θ^+ and adopt the suggestion that Θ^+ is a $K\pi N$ bound state. As one of the important in-medium properties of Θ^+ , the effective Θ^+ mass is also studied.

The paper is organized as follows. In the subsequent section, the general RMF theory for nuclear matter and a baryon in nuclear matter are discussed. Then a density dependent scalar coupling is introduce and a brief discussion of the effect to nuclear matter yields in in Sec. 3. The Kaon meson in nuclear medium is reviewed in Sec. 4. The effective mass and potential depth of Θ^+ with a new approach developed by us are discussed in Sec. 5. Finally a summary is given in Sec. 6.

2 A sketch of RMF theory in nuclear matter

In the RMF theory, the effective Lagrangian density for baryons can be written as

$$\begin{aligned} \mathcal{L} = \sum_B & (\bar{\Psi}_B (i\gamma^\mu \partial_\mu - M_B) \Psi_B - g_\sigma^B \bar{\Psi}_B \sigma \Psi_B - g_\omega^B \bar{\Psi}_B \gamma^\mu \omega_\mu \Psi_B \\ & - g_\rho^B \bar{\Psi}_B \gamma^\mu \rho_\mu^a \frac{\tau_a^B}{2} \Psi_B) + \frac{1}{2} \partial^\mu \sigma \partial_\mu \sigma - \frac{1}{2} m_\sigma^2 \sigma^2 - \frac{1}{3} g_2^2 \sigma^3 \\ & - \frac{1}{4} g_3^2 \sigma^4 - \frac{1}{4} \Omega^{\mu\nu} \Omega_{\mu\nu} + \frac{1}{2} m_\omega^2 \omega^\mu \omega_\mu - \frac{1}{4} R^{a\mu\nu} R_{\mu\nu}^a \end{aligned}$$

$$+\frac{1}{2}m_\rho^2\rho^{a\mu}\rho_\mu^a-\frac{1}{4}F^{\mu\nu}F_{\mu\nu}-e\bar{\psi}_B\gamma^\mu A^\mu\frac{1}{2}(1+\tau_3^B)\psi_B. \quad (1)$$

with

$$\begin{aligned}\Omega^{\mu\nu} &= \partial^\mu\omega^\nu - \partial^\nu\omega^\mu, \\ R^{a\mu\nu} &= \partial^\mu\rho^{a\nu} - \partial^\nu\rho^{a\mu}, \\ F^{\mu\nu} &= \partial^\mu A^\nu - \partial^\nu A^\mu.\end{aligned} \quad (2)$$

Here, \mathcal{L}_N is the standard Lagrangian of RMF^[31,32] for baryons. They involve baryons (Ψ_B), scalar meson fields (σ), vector mesons (ω_μ), vector isovector mesons (ρ_μ), and photons (A_μ). m_σ , m_ω , m_ρ , M_B and are the masses of σ , ω , ρ meson, baryon, respectively. g_σ^B , g_ω^B and g_ρ^B are the σ -baryon, ω -baryon and ρ -baryon coupling constants, respectively. The Pauli matrices for nucleons are written as τ_a^B with τ_3^B being the third component.

As an mean-field approximation, the equation of motion for a baryon is

$$(\gamma_\mu k^\mu - M_B - g_\sigma^B \sigma_0 - g_\omega^B \gamma^0 \omega_0 - g_\rho^B \gamma^0 \tau^3 \rho_{03})\psi_B = 0. \quad (3)$$

where σ_0 and ω_0 is the the mean-field values of scalar and vector mesons, respectively. The effective mass, M_B^* , of baryon is defined

$$M_B^* = M_B + g_\sigma^B \sigma_0. \quad (4)$$

For static, symmetric infinite nuclear matter, the equation of motion for the mean-field values of meson are written as

$$m_\sigma^2 \sigma_0 + g_2 \sigma_0^2 + g_3 \sigma_0^3 = \sum_B -g_\sigma^B \rho_s(B) \quad (5)$$

$$m_\omega^2 \omega_0 = \sum_B g_\omega^B \rho_B, \quad (6)$$

where $\rho_s(B) = \langle \bar{\psi}_B \psi_B \rangle$, $\rho_B = \langle \bar{\psi}_B \gamma^0 \psi_B \rangle$.

The density of energy, ε , for infinite nuclear mass reads

$$\varepsilon = \frac{1}{2}m_\sigma^2 \sigma_0^2 + \frac{1}{3}g_2 \sigma_0^3 + \frac{1}{4}g_3 \sigma_0^4 + \frac{1}{2}m_\omega^2 \omega_0^2 + \sum_B \varepsilon_B. \quad (7)$$

Here, ε_B is the density of energy for baryon and defined as

$$\varepsilon_B = \frac{2}{(2\pi)^3} \int_0^{k_F(B)} d\vec{k} (\vec{k}^2 + M_B^{*2})^{1/2}. \quad (8)$$

Combining the Eqs. (4), (7) and (8), we can obtain

$$\begin{aligned}\varepsilon(M_B^*) &= \frac{1}{2} \frac{m_\sigma^2 (M_B^* - M_B)^2}{(g_\sigma^B)^2} + \frac{1}{3} g_2 \frac{(M_B^* - M_B)^3}{(g_\sigma^B)^3} + \frac{1}{4} g_3 \frac{(M_B^* - M_B)^4}{(g_\sigma^B)^4} \\ &\quad + \frac{1}{2} m_\omega^2 \omega_0^2 + \frac{2}{(2\pi)^3} \sum_B \int_0^{k_F(B)} d\vec{k} (\vec{k}^2 + M_B^{*2})^{1/2}\end{aligned} \quad (9)$$

According to the relation, $\partial\varepsilon(M_B^*)/\partial M_B^* = 0$, it is easily obtained

$$M_B^* - M_B = -\left(\frac{g_\sigma^B}{m_\sigma}\right)^2 \left[\frac{g_2}{(g_\sigma^B)^3} (M_B^* - M_B)^2 + \frac{g_3}{(g_\sigma^B)^4} (M_B^* - M_B)^3\right]$$

$$+ \sum_B \frac{2}{(2\pi)^3} \int_0^{k_F(B)} d\vec{k} \frac{M_B^*}{(\vec{k}^2 + M_B^{*2})^{1/2}}] \quad (10)$$

If there is only a exotic baryon in symmetric infinite nuclear matter, the effect of a single exotic baryon on the mean field value can be neglected^[33]. Then

$$m_\sigma^2 \sigma_0 + g_2 \sigma_0^2 + g_3 \sigma_0^3 = g_\sigma^N (\rho_s(n) + \rho_s(p)) = -g_\sigma^N \rho_s \quad (11)$$

$$m_\omega^2 \omega_0 = g_\omega^N (\rho_n + \rho_p) = g_\omega^N \rho \quad (12)$$

$$M_N^* - M_N = -\left(\frac{g_\sigma^N}{m_\sigma}\right)^2 \left[\frac{g_2}{(g_\sigma^N)^3} (M_N^* - M_N)^2 + \frac{g_3}{(g_\sigma^N)^4} (M_N^* - M_N)^3 + \frac{4}{(2\pi)^3} \int_0^{k_F(N)} d\vec{k} \frac{M_N^*}{(\vec{k}^2 + M_N^{*2})^{1/2}} \right] \quad (13)$$

where $\rho_s(n)$ ($\rho_s(p)$) is the scalar density for neutron (proton), and ρ_n (ρ_p) is the baryon density for neutron (proton).

Comparing Eqs.(4) and (10), the mean-field value, σ_0 , reads

$$\sigma_0 = -\frac{g_\sigma^N}{m_\sigma^2} \left[\frac{g_2}{(g_\sigma^N)^3} (M_N^* - M_N)^2 + \frac{g_3}{(g_\sigma^N)^4} (M_N^* - M_N)^3 + \frac{4}{(2\pi)^3} \int_0^{k_F(N)} d\vec{k} \frac{M_N^*}{(\vec{k}^2 + M_N^{*2})^{1/2}} \right] \quad (14)$$

According to Eqs.(5),(14) and (17), the scalar density, ρ_s , is

$$\rho_s = \frac{4}{(2\pi)^3} \int_0^{k_F(N)} d\vec{k} \frac{M_N^*}{(\vec{k}^2 + M_N^{*2})^{1/2}} = \frac{M_N^*}{\pi^2} [k_F E_F^* - (M_N^*)^2 \ln(\frac{k_F + E_F^*}{M_N^*})] \quad (15)$$

where

$$E_F^* = ((M_N^*)^2 + k_F^2)^{1/2} \quad (16)$$

$$k_F = \left(\frac{3\pi^2 \rho_B}{2}\right)^{1/3} \quad (17)$$

Table 1: The parametrization of the nucleonic sector (adopted from Ref.^[6]). The masses are given in MeV and the coupling g_2 in fm⁻¹.

	M_N	m_σ	m_ω	m_ρ	g_σ^N	g_ω^N	g_ρ^N	g_2	g_3
NL-SH	939.0	526.059	783.0	763.0	10.444	12.945	4.383	-6.9099	-15.8337
NL3	939.0	508.194	782.501	763.0	10.217	12.868	4.474	-10.434	-28.885
Ref ^[34]	939.0	550	783.0		9.55	11.67			

2.1 The relation of $\sigma_0 - \rho_s$

In Eq.(11), if we let $g_2 = g_3 = 0$ (neglecting the nonlinear terms of σ_0), then

$$m_\sigma^2 \sigma_0 = g_\sigma^N \rho_s \quad (18)$$

which is an often used approximation in RMF calculation and more simple than the relation of Eq.(11). Can we neglect the nonlinear terms of σ_0 in calculating for infinite nuclear matter?

To understand it clearly, the mean-field value, σ_0/ρ_0 , as a function of nuclear scalar density, ρ_s/ρ_0 , in Eqs.(11) and (18) is shown in figure 1, respectively. Where ρ_0 is the saturation nuclear density, and let $\rho_0=0.15 \text{ fm}^3$ as the most used in RMF calculation.

For comparison, we use three sets of parameter NL-SH, NL3 and the parameters from Ref.^[34], which are listed in table 1. In figure 1, the red line (curve) is for NL3, black line (curve) is for NL-SH parameter set and blue line is for the parameters from Ref.^[34]; the solid line is obtained from Eq.(18)(neglecting the nonlinear terms of σ_0) and the dotted curve is obtained from Eq.(11)(including the nonlinear terms of σ_0).

From figure 1, we can see that there are obvious differences for the three parameter sets if we use Eq(18). When we consider effect from nonlinear terms of σ_0 and use the Eq. (11), the differences between the two parameter sets NL3 and NL-SH are nearly not visible in the region $\rho_s/\rho_0 < 1$, this implies in the low density region, there is little parameter dependence for the relation between σ_0 and ρ_s in Eq.(11). However, in higher density region, the differences between the two parameter sets NL3 and NL-SH are obvious. The results from Eq.(11) and (18) are quite different. There is only a simple linear relation for σ_0 and ρ_s in Eq.(18), however, σ_0 and ρ_s is a nonlinear relation in Eq.(11) and ρ_s has a limit, the maximum value ρ_{smax} is about $1.6\rho_0$ for NL3 set and $2.14\rho_0$ for NL-SH set. Even in the very low density region, the difference between Eq.(11) and (18) is obvious. Thus, the nonlinear terms of σ_0 can not be neglected in calculating, especially at high density.

As a conclusion, there is strong parameter dependence in the high density region and the nonlinear terms of σ_0 can affect the calculations obviously, the approximation $\sigma_0 = g_\sigma^N \rho_s / m_\sigma^2$ is indeed poor in RMF calculation, especially in dense medium.

By fitting the curve of Eq.(11) with NL3 parameter set, it yields

$$\sigma_0 = -0.15 \times (1.20058 \frac{\rho_s}{\rho_0} + 0.76387 (\frac{\rho_s}{\rho_0})^2 - 1.146 (\frac{\rho_s}{\rho_0})^3 + 0.50919 (\frac{\rho_s}{\rho_0})^4) fm^{-1} \quad (19)$$

with $\rho_s/\rho_0 < 1.6$.

And by fitting the curve of Eq.(11) with NL-SH parameter set, it yields

$$\sigma_0 = -0.15 \times (1.04793 \frac{\rho_s}{\rho_0} + 0.85141 (\frac{\rho_s}{\rho_0})^2 - 0.8515 (\frac{\rho_s}{\rho_0})^3 + 0.26773 (\frac{\rho_s}{\rho_0})^4) fm^{-1} \quad (20)$$

with $\rho_s/\rho_0 < 2.14$.

2.2 The relation of $\rho_s - \rho$

According to Eqs.(4),(15),(16) and (17), we can get

$$\begin{aligned} \rho_s = & \frac{M_N + g_\sigma^N \sigma_0}{\pi^2} [(\frac{3\pi^2 \rho_B}{2})^{1/3} ((M_N + g_\sigma^N \sigma_0)^2 + (\frac{3\pi^2 \rho_B}{2})^{2/3})^{1/2} \\ & - (M_N + g_\sigma^N \sigma_0)^2 \ln(\frac{(\frac{3\pi^2 \rho_B}{2})^{1/3} + ((M_N + g_\sigma^N \sigma_0)^2 + (\frac{3\pi^2 \rho_B}{2})^{2/3})^{1/2}}{M_N + g_\sigma^N \sigma_0})], \end{aligned} \quad (21)$$

Replace σ_0 here with the expressions in Eqs.(18), (19) and (20), the scalar density as a function of baryon density is deduced and shown in figure 2.

In figure 2, the blue curve is for Eq.(18), where the effect of the nonlinear terms of σ_0 is neglected and the parameter set is obtained from Ref.^[34]; the red and black curves is for relations (19) (NL3) and (20) (NL-SH), respectively, including the effect of the nonlinear terms of σ_0 .

From figure 2, it is found that the three curves are nearly no differences in the region $\rho/\rho_0 < 1$. Which indicates that the effect from nonlinear terms of σ_0 on the relations between ρ_s and ρ is small, and there is little parameter dependence in the region $\rho/\rho_0 < 1$. However, the three curves have obvious difference between each other in the region $\rho/\rho_0 > 1$. Thus, the effect from nonlinear terms of σ_0 on the relations between ρ_s and ρ should be included at high density. Comparing the red curve with the black curve, we find that there is strong parameter dependence in the high density region.

As a whole, in low density region such as $\rho/\rho_0 < 1$, the effect from nonlinear terms of σ_0 on the relations between ρ_s and ρ can be neglected and there is less parameter dependence; in high density region effect from nonlinear terms of σ_0 can not be neglected and there is strong parameter dependence. By fitting the black curve for NL-SH, it yields the simple relation

$$\frac{\rho_s}{\rho_0} = 0.95724\frac{\rho}{\rho_0} + 0.11603\left(\frac{\rho}{\rho_0}\right)^2 - 0.16357\left(\frac{\rho}{\rho_0}\right)^3 + 0.03448\left(\frac{\rho}{\rho_0}\right)^4 - 0.0022\left(\frac{\rho}{\rho_0}\right)^5, \quad (22)$$

where $\rho < 4\rho_0$. Similarly, the simple relation for NL3 parameter set in the region $\rho < 3\rho_0$ is

$$\frac{\rho_s}{\rho_0} = 0.88346\frac{\rho}{\rho_0} + 0.25674\left(\frac{\rho}{\rho_0}\right)^2 - 0.2382\left(\frac{\rho}{\rho_0}\right)^3 + 0.03782\left(\frac{\rho}{\rho_0}\right)^4, \quad (23)$$

2.3 Nucleon and Θ^+ effective mass in nuclear medium

For nucleon, the effective mass is

$$M_N^* = M_N + g_\sigma^N \sigma_0 \quad (24)$$

and for pentaquark Θ^+ , as studied in our previous work ^[12], the effective mass yields

$$M_{\Theta^+}^* = M_{\Theta^+} + \frac{4}{3}g_\sigma^N \sigma_0. \quad (25)$$

Combining the the Eqs.(20)/(19) and (22)/(23), the effective mass of a baryon as a function of ρ can be obtained.

In figure 3, the nucleon and Θ^+ effective masses as a function of nuclear density ρ are shown. The dashed and dash-dot curves correspond to Θ^+ and nucleon, respectively. For comparison, we show the results of both NL-SH and NL3 sets. The red curves are for NL-SH and black ones for NL3.

From the figure, it is shown that at normal nuclear density ρ_0 the nucleon effective mass $M_N^*/M_N \simeq 0.59$, which consists with the initial setting for NL-SH and NL3, $M_N^*/M_N \simeq 0.6$; and the Θ^+ effective mass $M_{\Theta^+}^*/M_{\Theta^+} \simeq 0.67$.

It is easily found that both of the parameter sets, NL3 and NL-SH, give the similar results in the region $\rho/\rho_0 < 1.4$, but when $\rho/\rho_0 > 1.5$ the results for them are very different. At $\rho = 2.5\rho_0$ the difference of effective mass of nucleon between the two parameter sets is about $0.03M_N=28$ MeV; and for Θ^+ , the difference is about 38.5 MeV. Thus, in high density region, we must be careful in selecting the proper parameter set for calculating.

3 Density dependent coupling $g_\sigma^N(\sigma_0)$ and the effect to nuclear matter

From the analysis in section 2, we know there is strong parameter dependence for nuclear matter in high density region. That is, the coupling constants are of the essence for predicting

the properties of nuclear matter in high density region. However, the couplings may be no longer constants in this region and change with density. The reason is that the quark freedom has the most possibility to appear in high density nuclear matter, which affects the couplings. Thus, it is necessary to consider the couplings as a function of density. In fact, the density dependent meson-nucleon coupling has been suggested in Refs.^[36,37] and studied such as in Ref.^[38].

3.1 Density dependent coupling

In the framework of RMF, the nucleons are considered as structureless, however, in high density matter there maybe appear quark freedom. Thus, it is necessary to consider the effect from the quark structure of nucleon. Which has been investigated in QMC model^[35]. According to the QMC model, the contribute of quark structure of nucleon can be included in the scalar coupling only and does not affect the vector meson coupling. The difference between RMF and QMC lies only in the scalar coupling g_σ^N , which is a function of meson field σ in QMC, while in RMF the coupling g_σ^N is a constant. In present work we attempt to extent the coupling $g_\sigma^N(\sigma_0)$ in QMC model to RMF.

According to QMC model, the coupling g_σ^N is written as^[33,35]

$$g_\sigma^N(\sigma_0) = g_\sigma^N|_{\sigma=0} C_N(\sigma_0), \quad (26)$$

where $C_N(\sigma_0)$ is a function of σ_0 , if we let $C_N(\sigma_0) = 1$, then QMC model is no difference between RMF. As a well approximation up to three times normal nuclear density, $3\rho_0$, the the coupling g_σ^N yields^[33]

$$g_\sigma^N(\sigma_0) = g_\sigma^N|_{\sigma=0} (1 + \frac{a_N}{2} g_\sigma^N|_{\sigma=0} \sigma_0), \quad (27)$$

which changes linearly with the scalar meson field. where $a_N = 8.8 \times 10^{-4} \text{ MeV}^{-1}$.

If we consider the effect from the internal structure of nucleon in RMF as well as QMC model, it is reasonable to believe that the scalar coupling g_σ^N also changes with the scalar meson field in RMF, and has the same form as Eq.(27). Thus, the differences between QMC model and RMF model lie only in the constants $g_\sigma^N|_{\sigma=0}$ and a_N .

Now we roughly estimate the values for $g_\sigma^N|_{\sigma=0}$ and a_N in RMF. Generally, the effective mass of nucleon at normal nuclear density is about $0.8M_N$ in QMC, however, which is $0.6M_N$ in RMF. Thus, the mass shift $M_N - M_N^* = -g_\sigma^N \sigma = 0.2, 0.4M_N$ for QMC and RMF model at normal nuclear density, respectively. As an approximation, $g_\sigma^N|_{\sigma=0} \approx g_\sigma^N$, then $-g_\sigma^N|_{\sigma=0} \sigma \approx 0.2, 0.4M_N$ for QMC and RMF model at normal nuclear density, respectively. For both models at the same value of scalar field σ , the change ratio should be the same. Namely, $(a_N/2g_\sigma^N|_{\sigma_0=0}\sigma_0|_{\rho_0})_{QMC} = (a_N/2g_\sigma^N|_{\sigma_0=0}\sigma_0|_{\rho_0})_{RMF}$. Combining the analysis above, we easily obtain $a_N \simeq 4.4 \times 10^{-4} \text{ MeV}^{-1}$ for RMF, which is one half of that of QMC model.

Next, we will determine $g_\sigma^N|_{\sigma=0}$. In RMF, the effective mass $M_N^* \simeq 0.6M_N$ at normal nuclear density. It is one of the characters for nuclear matter in RMF and should not change at normal nuclear density, although we introduce the density dependent coupling $g_\sigma^N(\sigma_0)$. To satisfy the condition, it only needs $g_\sigma^N = g_\sigma^N(\sigma_0|_{\rho_0})$. Then, the coupling constant $g_\sigma^N|_{\sigma_0=0}$ can be determined at once according to the relation

$$g_\sigma^N = g_\sigma^N|_{\sigma_0=0} (1 + \frac{a_N}{2} g_\sigma^N|_{\sigma_0=0} \sigma_0|_{\rho_0}). \quad (28)$$

For NL-SH set, $g_\sigma^N=10.444$, then the corresponding value $g_\sigma^N|_{\sigma=0}=11.48$ and for NL3 set, $g_\sigma^N=10.217$, the value $g_\sigma^N|_{\sigma=0}=11.24$.

Now, the scalar coupling $g_\sigma^N(\sigma_0)$ as a function of σ_0 is obtained. It is necessary to study how much it affects on the properties of nuclear matter in RMF. Thus, we reanalyse the relations $\sigma_0 - \rho_s$ and $\rho_s - \rho$ and study the effect on the nucleon and Θ^+ effective masses.

3.2 Effect on the relation $\sigma_0 - \rho_s$

Together with the determined value for $g_\sigma^N|_{\sigma=0}$, a_N and combining the Eqs.(11), and (27), the scalar meson mean-field value, σ_0 , as a function nuclear density ρ can be easily obtained. Here, we use NL-SH parameter set, $g_\sigma^N|_{\sigma=0}=11.48$, as an example, the relation $\sigma_0 - \rho_s$ is shown in figure 4. For comparison, we also show the relation, $\sigma_0 - \rho_s$, of constant coupling NL-SH set.

In figure 4, the red and black curves correspond to the density dependent coupling $g_\sigma^N(\sigma)$ and the constant coupling, respectively. From figure 4, it is seen that the absolute value of σ_0 for the density dependent coupling $g_\sigma^N(\sigma)$ is a little larger than that of constant coupling in the region $\rho_s/\rho_0 < 1$, the difference is nearly not visible. However, in the region $\rho_s/\rho_0 > 1$, it gives very different results for the two case, especially in higher scalar density region. The curve for density dependent coupling is driven down and moves to higher density region. The maximum of scalar density for density dependent coupling $((\rho_s/\rho_0)_{max} \simeq 2.75)$ is larger than that of constant coupling $((\rho_s/\rho_0)_{max} \simeq 2.14)$.

By fitting the curve for the considered density dependent coupling $g_\sigma^N(\sigma)$ in the region $\rho_s/\rho_0 < 2.5$, we get the following relation

$$\sigma_0 = -0.15 \times (1.59484 \frac{\rho_s}{\rho_0} - 0.37443 (\frac{\rho_s}{\rho_0})^2 + 0.10156 (\frac{\rho_s}{\rho_0})^3) fm^{-1} \quad (29)$$

3.3 Effect on the relation $\rho_s - \rho$

If we replace the constant coupling g_σ^N with the density dependent coupling $g_\sigma^N(\sigma)$ in Eq.(21), combining the Eq.(29), a new relation between ρ_s and ρ is obtained at once.

In figure 5, ρ_s as a function of ρ is plotted. Where we adopts NL-SH parameter set. The red curve is for constant coupling, and the black curve is for the density dependent coupling. In figure 5, it is found that there is nearly no difference in the region $\rho/\rho_0 < 1.4$ between the two curves, which agrees with the conclusion in subsection 2.2 that there is less parameter dependence in low density region. However, it is shown obvious difference ($\sim 0.2\rho_0$) in the region $2 \sim 3\rho_0$, when considering the density dependent coupling, the scalar density, ρ_s becomes larger. Compared with the scalar density of constant coupling, the scalar density of density dependent coupling is enhanced about 12% ($0.2\rho_0$) at $\rho = 3\rho_0$.

By fitting the curve of the density dependent coupling $g_\sigma^N(\sigma)$ in the region $\rho/\rho_0 < 3$, the relation between ρ_s and ρ also yields

$$\frac{\rho_s}{\rho_0} = 1.05695 \frac{\rho}{\rho_0} - 0.09344 (\frac{\rho}{\rho_0})^2 - 0.01157 (\frac{\rho}{\rho_0})^3 \quad (30)$$

3.4 The relation $g_\sigma^N(\sigma_0) - \rho$

Now, combining the Eqs.(27),(29) and (30), the coupling $g_\sigma^N(\sigma_0)$ as a function of ρ is easily obtained, which is shown in figure 6. From figure 6, we can see the couplings $g_\sigma^N(\sigma)$ how to

change with the nuclear density clearly. For NL-SH set, the coupling $g_\sigma^N(\sigma)$ changes in the region $0.89 \sim 1.1g_\sigma^N$ when $\rho < 3\rho_0$. Namely, considering the effect of density the change of the scalar coupling is about within $\pm 10\%$. If the nuclear density larger than normal nuclear density, the coupling is a littler smaller than g_σ^N , and if the nuclear density lower than normal nuclear the density dependent coupling will be a little larger than g_σ^N .

3.5 Effect on nucleon and Θ^+ effective mass

Finally, to understand the density dependent coupling $g_\sigma^N(\sigma)$ how to affect the baryon effective mass in nuclear medium, we show the nucleon and Θ^+ effective mass as a function of nuclear density, ρ in figure 7. Which is easily obtained by replace the constant coupling g_σ^N with the density dependent coupling $g_\sigma^N(\sigma)$ in Eqs.(24) and (25) and combining the relations (29), (30). For comparison, the nucleon and Θ^+ effective masses as a function of nuclear density, ρ with the constant coupling g_σ^N are also plotted in figure 7.

For simplify, we only use the NL-SH parameter set as an example. In figure 7, the red curves are for the density dependent coupling and black curves are for the constant coupling; the dashed curves are for Θ^+ and dash-dot curves are for nucleon.

From figure 7, we can see that if we use the density dependent coupling, the ratios of the effective mass of nucleon or Θ^+ to those in free space (M^*/M) become larger in the region $\rho > \rho_0$. The nucleon and Θ^+ effective masses are enhanced $0.05M_N \simeq 47$ MeV and $0.04M_{\Theta^+} \simeq 62$ MeV at $\rho = 3\rho_0$, respectively. Which indicates that the interaction between scalar meson and baryon is obviously depressed by the density dependent coupling in the high density region. On the other hand, in the low density region $\rho < \rho_0$, the ratios are smaller than those of constant coupling, the maximum difference appears at $\rho \simeq 0.5\rho_0$, where the nucleon and Θ^+ effective masses are dressed about $0.03M_N \simeq 28$ MeV and $0.025M_{\Theta^+} \simeq 38$ MeV, respectively.

As a whole, the density dependent coupling $g_\sigma^N(\sigma)$ has strong effect on the properties of nuclear matter, especially in higher density region. According our analysis, the coupling should be serious considered with the RMF framework, especially in the region $\rho > 1.5\rho_0$. We must point out that it is only an attempt to introduce the density dependent coupling $g_\sigma^N(\sigma)$ in RMF and far from precise calculation still.

4 Kaon meson in nuclear medium

4.1 RMF approach

Kaons were incorporated into the RMF model by using kaon-nucleon interactions motivated by one meson exchange models^[9, 39]. In the meson-exchange picture, the scalar and vector interaction between kaon and nucleon are mediated by the exchange of σ and ω meson, respectively. For symmetric nuclear matter, the simplest kaon-meson interaction Lagrangian can be written as

$$\mathcal{L}_k = \partial_\mu \bar{K} \partial^\mu K - m_k^2 \bar{K} K - g_{\sigma k} m_k \bar{K} K \sigma - ig_{\omega k} (\bar{K} \partial_\mu K \omega^\mu - K \partial_\mu \bar{K} \omega^\mu) + (g_{\omega k} \omega_\mu)^2 \bar{K} K, \quad (31)$$

where σ and ω^μ are the scalar and the vector fields, respectively. $g_{\sigma k}$ and $g_{\omega k}$ are the coupling constants between kaon and the scalar and the vector fields, respectively. The

coupling constants to the vector mesons are chosen from the SU(3) relation assuming ideal mixing^[9]

$$2g_{\omega k} = 2g_{\pi\pi\rho} = 6.04. \quad (32)$$

The coupling constants to scalar meson can be given by fitting the KN scattering lengths in experiments^[39, 40]

$$g_{\sigma k} \approx 1.9 \sim 2.3 \approx 1/5 g_{\sigma}^N. \quad (33)$$

In the mean-field approximation, the equation of motion for kaons reads

$$\{\partial_\mu \partial^\mu + m_k^2 + g_{\sigma k} m_k \sigma_0 + 2g_{\omega k} \omega^0 i \partial^\mu - (g_{\omega k} \omega^0)^2\} K = 0, \quad (34)$$

where σ_0 is the mean-field value of scalar field and ω^0 is the time-component of vector field. Decomposing the kaon field into plan waves, one obtains the equation for the kaon (antikaon) energy ω and momentum k

$$-\omega^2 + k^2 + m_k^2 + g_{\sigma k} m_k \sigma_0 + 2g_{\omega k} \omega^0 \omega - (g_{\omega k} \omega^0)^2 = 0, \quad (35)$$

The energies of kaon and antikaon in nuclear medium are then given by

$$\omega_k = [m_k^{*2} + k^2]^{1/2} + g_{\omega k} \omega^0, \quad (36)$$

$$\omega_{\bar{k}} = [m_k^{*2} + k^2]^{1/2} - g_{\omega k} \omega^0, \quad (37)$$

where the effective kaon mass is

$$m_k^* = \sqrt{m_k^2 + g_{\sigma k} m_k \sigma_0}. \quad (38)$$

From the in-medium dispersion relations (34), (35), the kaon and antikaon potential can be defined as^[41, 42]

$$U_{K, \bar{K}} = \omega_{k, \bar{k}} - \sqrt{m_k^2 + k^2} \quad (39)$$

4.2 Chiral approach

For symmetric nuclear matter, the effect of isospin is neglected. Following the outline in Refs.^[39, 43], the kaon-nucleon chiral Lagrangian is written as

$$\mathcal{L}_{KN}^{chiral} = -\frac{3i}{8f_k^2} \bar{N} \gamma^\mu N [\bar{K} \partial^\mu K - (\partial^\mu \bar{K}) K] + \frac{\Sigma_{KN}}{f_k^2} \bar{N} N \bar{K} K + \frac{\tilde{D}}{f_k^2} \bar{N} N (\partial_\mu \bar{K} \partial^\mu K) \quad (40)$$

where $f_k \approx 93$ MeV is the kaon decay constant and Σ_{KN} is the KN sigma term. The first term corresponds to the Tomozawa-Weinberg vector interaction. The next term is the scalar interaction which will shift the effective mass of the kaon and the antikaon. The last term, which sometimes is called off-shell term, also modify the scalar interaction. Σ_{KN} is not known very well, in the original work, it was chose $\Sigma_{KN} \approx 2m_\pi$ in accordance with the Born model^[43]. More recently, the value $\Sigma_{KN} \approx 450$ MeV is favored according to lattice gauge calculations^[44]. Thus, it may vary in the region 270 MeV to 450 MeV. By fitting the KN scattering lengths, one can determine the constant^[39]

$$\tilde{D} = 0.33/m_k - \Sigma_{KN}/m_k^2 \quad (41)$$

The equation of motion for kaon field in the mean-field approximation and in uniform matter reads

$$\{\partial_\mu \partial^\mu + m_k^2 - \frac{\Sigma_{KN}}{f_k^2} \rho_s + \frac{\tilde{D}}{f_k^2} \rho_s \partial_\mu \partial^\mu + \frac{3i}{4f_k^2} \rho_N \partial_t\} K = 0 \quad (42)$$

where $\rho_s = \langle \bar{N}N \rangle$ is the scalar density and $\rho_N = \langle N^\dagger N \rangle$ is the vector density for nucleons. Plan wave decomposition of the equation of motion yields

$$-\omega^2 + k^2 + m_k^2 - \frac{\Sigma_{KN}}{f_k^2} \rho_s - \frac{\tilde{D}}{f_k^2} \rho_s (\omega^2 - k^2) - \frac{3}{4f_k^2} \omega \rho_N = 0, \quad (43)$$

The energy of kaon (antikaon) in the nuclear medium is

$$\omega_K = \{[(m_k^{*2} + k^2)(1 + \frac{\tilde{D}}{f_k^2} \rho_s)^2 + (\frac{3}{8f_k^2} \rho_N)^2]^{1/2} + \frac{3}{8f_k^2} \rho_N\} (1 + \frac{\tilde{D}}{f_k^2} \rho_s)^{-1}, \quad (44)$$

$$\omega_{\bar{K}} = \{[(m_k^{*2} + k^2)(1 + \frac{\tilde{D}}{f_k^2} \rho_s)^2 + (\frac{3}{8f_k^2} \rho_N)^2]^{1/2} - \frac{3}{8f_k^2} \rho_N\} (1 + \frac{\tilde{D}}{f_k^2} \rho_s)^{-1}, \quad (45)$$

where m_k^{*2} is the kaon effective mass

$$m_k^* = \sqrt{(m_k^2 - \Sigma_{KN} \rho_s / f_k^2) / (1 + \tilde{D} \rho_s / f_k^2)} \quad (46)$$

4.3 Results

According to Eqs.(36) or (44), the Kaon energy ω_K (at the momentum $k = 0$) as a function of nuclear density ρ is easily obtain with the relations in section 2. Figure 8 shows the Kaon energy ω_K of both RMF method (Eq.(36)) and ChPT approach (Eq.(44)). For RMF approach, we list the results of NL-SH and NL3 parameter sets, the result of density dependent scalar coupling (NL-SH) is also plotted in the same figure. And for ChPT approach, we consider three cases: $\Sigma_{KN} = 270, 350, 450$ MeV, the relation $\rho_s - \rho$ obtains from Eq.(22), which is for NL-SH parameter set.

As seen in figure 8, all the models show a quite similar behavior in the low density region $\rho < \rho_0$. The results of the model of density dependent scalar coupling (NL-SH) are a little lower (less than 2.5 MeV) than those of ChPT approach. It should be noted that the results for ChPT approach is also a little lower than those of RMF with constant coupling in the low density region. Which indicates that the trend for density dependent scalar coupling (NL-SH) agrees with ChPT approach in this region. From the figure, we also find that the effect from considering density dependence for scalar coupling is within 4 MeV for kaon energy ω_K in the region $\rho < \rho_0$. In this region, the ChPT approach always gives larger kaon energy than that of RMF (constant coupling) approach. When we consider density dependence for scalar coupling in RMF approach, the Kaon energy is enhanced in the region $\rho > \rho_0$ and the result of RMF is compatible with the ChPT approach's. As seen in figure 8, the curve for density dependent scalar coupling (NL-SH) is very close the curve for $\Sigma_{KN} = 270$ in the region $\rho > \rho_0$. Which indicates that the RMF model considered density dependent coupling is consistent with ChPT model in a certain extent. At $\rho = \rho_0$, the kaon energy $\omega_K = 527$ MeV for RMF and ChPT, except $\omega_K = 532$ MeV for ChPT ($\Sigma_{KN} = 450$). As defined in Eq.(39), the potential of kaon is $U_K = 33$ MeV for RMF model and $U_K = 28 \sim 33$ MeV

for ChPT model at normal nuclear density, which is compatible with kaon optical potential $U_{opt}^{KN} \approx 29$ MeV^[39] at normal nuclear density. At $\rho = 3\rho_0$ the kaon energy $\omega_K = 630$ MeV for NL3 ($\omega_K = 630$ MeV for NL-Z in Ref.^[39]), $\omega_K = 633$ MeV for NL-SH and $\omega_K = 640$ MeV for density dependent coupling in RMF model and $\omega_K = 645 \sim 690$ MeV ($\omega_K = 630 \sim 670$ MeV in Ref.^[39]) for ChPT model. All the results are compatible with the calculation in Ref.^[39] as a whole.

5 Θ^+ as a $K\pi N$ bound state in RMF

what we discuss in the above section 2, 3 and in our previous work^[12] is not considered the structure of Θ^+ and roughly think it is a point-like particle in RMF. However, Θ^+ has the most possibility that it is a bound state of several quark clusters such as diquark-triquark $(ud\bar{s})(ud)$ structure suggested by Lipkin^[45, 46] or $K\pi N$ molecule state discussed in Refs.^[47–49]. If Θ^+ is a bound state of, such as, $K\pi N$, its properties may be very different from that of point-like one in RMF. To understand the effect of structure on the in-medium properties of Θ^+ , in the following work, we will assume Θ^+ as a $K\pi N$ bound state and discuss its properties in nuclear medium within the framework of RMF.

According to the idea of meson-exchange model, a $K\pi N$ system interacts with nucleon by exchanging meson can be looked as K , π and N exchanging meson with nucleon, respectively. Thus, the investigation of the interaction between Θ^+ and nucleon in medium turns to investigate the interaction KN , πN and NN in medium. We can assume that the pions as Goldstone bosons do not change their properties in the medium^[50]. Thus, we neglect the πN interaction in medium.

In RMF, the interactions between hadron are mediated by the exchange of scalar meson σ and vector meson ω . The effective Lagrangian for Θ^+ reads

$$\mathcal{L}_{\Theta^+} \simeq \mathcal{L}_K + \mathcal{L}_N + \mathcal{L}_\pi + \mathcal{L}_0, \quad (47)$$

where \mathcal{L}_K , \mathcal{L}_N and \mathcal{L}_π is the effective Lagrangian for nucleon and kaon and pion, respectively, and \mathcal{L}_0 is for the internal interaction of $K\pi N$ system, which is a constant. There, we need not know \mathcal{L}_π for our present discussion because we neglect the πN interaction in medium. According to the review in section 2, \mathcal{L}_N and \mathcal{L}_K can be written as

$$\mathcal{L}_N = \bar{\Psi}_N(i\gamma^\mu \partial_\mu - M_N)\Psi_N - g_\sigma^N \bar{\Psi}_N \sigma \Psi_N - g_\omega^N \bar{\Psi}_N \gamma^\mu \omega_\mu \Psi_N, \quad (48)$$

$$\begin{aligned} \mathcal{L}_K = & \partial_\mu \bar{K} \partial^\mu K - m_k^2 \bar{K} K - g_{\sigma k} m_k \bar{K} K \sigma \\ & - i g_{\omega k} (\bar{K} \partial_\mu K \omega^\mu - K \partial_\mu \bar{K} \omega^\mu) + (g_{\omega k} \omega_\mu)^2 \bar{K} K, \end{aligned} \quad (49)$$

The in-medium energy of nucleon is then given by

$$E_N(p) = \sqrt{(M_N + g_\sigma^N \sigma_0)^2 + p^2} + g_\omega^N \omega_0 \quad (50)$$

and the in-medium energy of Θ^+ is

$$E_{\Theta^+} = E_N(p) + \omega_k + E_\pi + B \quad (51)$$

where $E_\pi = \sqrt{m_\pi^2 + p^2}$ is the energy for pion and B is the bound energy of $K\pi N$ system, both of them are not change in nuclear medium. For zero momentum, the in-medium of Θ^+ energy is given by

$$E_{\Theta^+} = M_{\Theta^+}^* + g_\omega^N \omega_0 + g_{\omega k} \omega_0. \quad (52)$$

where the effective Θ^+ mass $M_{\Theta^+}^*$ in nuclear matter is

$$M_{\Theta^+}^* = M_N^* + m_k^* + m_\pi + B. \quad (53)$$

In free space, the Θ^+ mass is $M_{\Theta^+} = M_N + m_k + m_\pi + B$, combining Eqs.(24, 38) the Θ^+ effective mass can be written as

$$M_{\Theta^+}^* = M_{\Theta^+} + g_\sigma^N \sigma_0 + \sqrt{m_k^2 + g_{\sigma k} m_k \sigma_0} - m_k \quad (54)$$

The potential of Θ^+ can be defined as the difference between its energies in the medium and in free space

$$U_{\Theta}^{K\pi N}(p, k) = E_N(p) + \omega_k - \sqrt{M_N^2 + p^2} - \sqrt{m_k^2 + k^2} \quad (55)$$

Thus, the potential of Θ^+ for zero momentum $U_{\Theta}^{K\pi N}(p, k = 0)$ is

$$\begin{aligned} U_{\Theta}^{K\pi N} &= g_\sigma^N \sigma_0 - g_\omega^N \omega_0 + [m_k^2 + g_{\sigma k} m_k \sigma_0]^{1/2} + g_{\omega k} \omega^0 - m_k \\ &= U_N(p = 0) + U_K(k = 0), \end{aligned} \quad (56)$$

where $U_N(p = 0) = g_\sigma^N \sigma_0 - g_\omega^N \omega_0$ is the relativistic potential of nucleon and $U_K(k = 0) = [m_k^2 + g_{\sigma k} m_k \sigma_0]^{1/2} + g_{\omega k} \omega^0 - m_k$ is the potential of kaon for zero momentum.

5.1 $K\pi N$ bound state effective mass

The effective masses defined in Eq.(54) are plotted in figure 9 for NL-SH, NL3 and density dependent coupling sets, respectively. For comparison, we also plot the effective masses defined in Eq.(25) in the same figure. The blue curves is for Θ^+ as $K\pi N$ bound state and black curves is for Θ^+ as a structureless particle in RMF. The two models give very different results. At normal nuclear density, the effective mass $M_{\Theta^+}^* \simeq 0.73M_{\Theta^+} = 1120$ MeV for $K\pi N$ bound state and the model for structureless particle gives much smaller result, $M_{\Theta^+}^* \simeq 0.67M_{\Theta^+} = 1030$ MeV. The Θ^+ effective mass is enhanced 90 MeV (6% M_{Θ^+}) by considering the structure. As seen in figure 9, there are more obvious differences at higher nuclear density between two models. At $\rho = 3\rho_0$, the $K\pi N$ bound state effective mass $M_{\Theta^+}^* \simeq 770, 720, 705$ MeV and the structureless Θ^+ effective mass $M_{\Theta^+}^* \simeq 610, 550, 540$ MeV for the density dependent coupling, NL-SH and NL3 set, respectively; the results for $K\pi N$ bound state are enhanced about 160 MeV comparing with those of non-structure Θ^+ for the same parameter set. From the figure, we also find that for $K\pi N$ bound state, using the density dependent coupling the effective masses are enhanced at $\rho > \rho_0$, the enhanced mass is 50 ~ 60 MeV around the region $2.5\rho_0 \sim 3\rho_0$. There is strong parameter dependence in the region $\rho > 1.5\rho_0$, the mass difference is about 10 ~ 30 MeV between NL-SH and NL3 set, however, in the low density region $\rho < 1.5\rho_0$, there is nearly no visible difference between the two curves (NL-SH and NL3). If considering the effect of density dependent coupling, the effective mass is obviously dressed in the region $\rho < \rho_0$, the most dressed mass is about 30 MeV at $\rho \approx 0.5\rho_0$.

As a conclusion, the effective mass of Θ^+ strongly depends on its internal structure considered in RMF, the difference is up to 90 MeV between $K\pi N$ bound state and structureless Θ^+ at $\rho = 3\rho_0$; the density dependent coupling can also strongly affect the effective mass in the whole region, especially at high density; there is little parameter dependence for effective mass in the low density region, however, in high density region, the effect is also obvious.

5.2 Potential depth for Θ^+ in nuclear medium

We also give the relativistic potential of Θ^+ in figure 10. For comparison, the potential of nucleon is also show according to the equation $U_N = g_\sigma^N \sigma_0 - g_\omega^N \omega_0$. The blue, black, red curves are for Θ^+ as $K\pi N$ bound state, point-like Θ^+ and nucleon, respectively. The dash-dot, dashed and dotted curves are for density dependent coupling, NL-SH and NL3 set, respectively.

For NL-SH and NL3 parameter sets, the curves are very similar in the region $\rho < 1.2\rho_0$, however, they show strong parameter dependence in the higher density region $\rho > 1.2\rho_0$. The minima of potential depth appear at $\rho \simeq 1 \sim 1.2\rho_0$. For $K\pi N$ bound state, the potential depth $U_{\Theta^+}^{K\pi N} \simeq -37.5$ MeV at around normal nuclear density, which is very close the Θ^+ potential $U = -40$ MeV of QCD Sum Rule which remains independent of a parameter y [29]. For nucleon, the relativistic potential depth $U_N \simeq -65$ MeV. The deepest potential is for Θ^+ (structureless), $U_{\Theta^+} \simeq -90$ MeV, which is investigated in our previous work [12]. Comparing the potential depth for $K\pi N$ bound state and point-like Θ^+ , we find that if we consider the Θ^+ as $K\pi N$ bound state the potential depth will be much shallower, however, it is still strong enough to form Θ^+ bound states in nuclei according to our calculation in Ref. [12]. If Θ^+ as a $K\pi N$ bound state is the case, according to our prediction, the notion suggested in Ref. [26, 28] of strong binding for Θ^+ in nuclei will be modified.

The curves for density dependent coupling give much deeper potentials than those of NL-SH and NL3 parameter sets in $\rho < \rho_0$, and much higher potentials in the high density region $\rho > 1.2\rho_0$. The potential minimum appears at low density $\rho \simeq 0.6\rho_0$. For $K\pi N$ bound state, the relativistic potential depth $U_{\Theta^+min}^{K\pi N} \simeq -60$ MeV, for nucleon, $U_{Nmin} \simeq -75$ MeV, and for Θ^+ , $U_{\Theta^+min} \simeq -110$ MeV. The reason for deeper depth of the relativistic potential at $\rho \simeq 0.6\rho_0$ is that the scalar coupling g_σ^N becomes larger in $\rho < \rho_0$ than that of normal density and the vector coupling g_ω^N is not change. If the prediction is the truth, the strongest binding for baryons such as Θ^+ , nucleon will appear at lower density than normal density and the binding will be stronger. For the potential also depend another coupling constant g_ω^N , whether the density affect the strength of the vector coupling or not is not known, it is still a challenge for our prediction.

6 Summary

In this paper, we have carefully discussed the symmetric nuclear matter in RMF and obtain the relation $\sigma_0 - \rho_s$ and $\rho_s - \rho$ for NL-SH and NL3 parameter sets. From the analysis, we find that $\sigma_0 \simeq g_\sigma^N \rho_s / m_\sigma^2$ is a rather poor approximation in RMF calculation, the nonlinear scalar self-interaction term can strongly affect the result, especially at higher density. It is also found that there are strong parameter dependence in higher density region, however, the effect in the region $\rho < \rho_0$ can be neglected. With the the relation $\sigma_0 - \rho_s$ and $\rho_s - \rho$, we analyse the effective mass for nucleon and the Θ^+ studied in our previous work [12], how the effective masses of them change with the nuclear density is plotted. At normal nuclear density the effective mass for Θ^+ is $M_{\Theta^+}^* = 0.67M_{\Theta^+}$.

According to the idea of QMC model, we have attempted to introduce a density dependent scalar coupling $g_\sigma^N(\sigma_0)$. In which, two parameters are roughly determined as $a_N \simeq 4.4 \times 10^{-4}$ MeV⁻¹ and $g_\sigma^N|_{\sigma=0} = 11.48, 11.24$ for NL-SH and NL3 set, respectively. Then, we re-discussed the $\sigma_0 - \rho_s$ and $\rho_s - \rho$ with density dependent scalar coupling $g_\sigma^N(\sigma_0)$. We find that the density dependent coupling $g_\sigma^N(\sigma_0)$ affect the relations $\sigma_0 - \rho_s$ and $\rho_s - \rho$

very little in the region $\rho < \rho_0$, however, its effect is obvious at higher density. The effect on baryon effective masses in low density region $\rho < \rho_0$ can not be neglected, the largest effect is about $2 \sim 3\%$ baryon mass lower than that of constant coupling, and at $\rho = 3\rho_0$ the nucleon and Θ^+ effective masses are enhanced 47 and 62 MeV, respectively. As a whole, it is very necessary to consider the density dependent coupling in RMF, in present work it only an attempt to consider the density dependent scalar coupling $g_\sigma^N(\sigma_0)$, how to accurate the parameters a_N and $g_\sigma^N|_{\sigma=0}$ is a problem which should be solved in future work.

We also review the theory of Kaon meson in RMF and ChPT. According to our investigation in section 2, the energy of K^+ in nuclear medium at momentum $k = 0$ is shown in figure 8 for both RMF and ChPT methods. Our results is consistent with those of Ref.^[39] with NL-Z parameter set. The potential depth is $U_K \simeq 33$ MeV for RMF model and $U_K = 28 \sim 33$ MeV for ChPT model at normal nuclear density. The energy of K^+ for density dependent coupling seems more close to that of ChPT method, especially in the region $\rho > \rho_0$. Which indicates that the RMF model considered density dependent coupling is consistent with ChPT model in a certain extent.

The most interesting point is that we develop another approach in RMF to study Θ^+ . Where Θ^+ is look as a $K\pi N$ bound state and the interaction between nucleons are approximated to the interaction of NN and KN in RMF. The effective mass is $M_{\Theta^+}^* \simeq 0.73M_{\Theta^+}=1120$ MeV at normal density, which is much larger than $M_{\Theta^+}^* \simeq 0.67M_{\Theta^+}=1030$ MeV as a non-structure particle in RMF^[12]. The potential depth is $U_{\Theta^+}^{K\pi N} \simeq -37.5$ MeV much shallower than $U_{\Theta^+} \simeq -90$ MeV as a non-structure particle in RMF^[12] at normal density. The density dependent coupling also strongly affects the potential depth, it gives much deeper potential depth in low density region $\rho < \rho_0$, much larger potential $\rho > 1.2\rho_0$. If it is the case the deepest bound state will appear at $\rho < \rho_0$. For the potential also depends another coupling constant g_ω^N , whether the density affect the strength of the vector coupling or not is not known, it is still a challenge for our prediction.

References

- [1] K. Saito and A. W. Thomas, Phys. Rev. C **51**, 2757(1995).
- [2] F. Kling, T. Waas and W. Weise, Phys. Lett. B **431**, 254 (1998).
- [3] H. Shen, S. Tamenaga and H. Toki, Nucl. Phys. A **745**, 121 (2004).
- [4] T. Hatsuda, Su H. Lee, Phys. Rev. C **46**, R34 (1992).
- [5] M. Rufa, P.-G. Reinhard et al., Phys. Rev. C **38**, 390(1988).
- [6] G. A. Lalazissis, J. König, and P. Ring, Phys. Rev. C **55**, 540(1997).
- [7] M. Rufa, J. Schaffner et al., Phys. Rev. C **42**, 2469(1990).
- [8] J. Mareš and B. K. Jennings, Phys. Rev. C **49**, 2472(1994).
- [9] Jürgen Schaffner and Igor N. Mishustin, Phys. Rev. C **53**, 1416(1996).
- [10] Y. H. Tan, Y. A. Luo, P. Z. Ning and Z. Y. Ma, Chin. Phys. Lett. **18**, 1030 (2001).
- [11] Y. H. Tan, X. H. Zhong, C. H. Cai and P. Z. Ning, Phys. Rev. C **70**, 054306(2004).
- [12] X. H. Zhong, Y. H. Tan et al., arXiv:nucl-th/0408046 (to appear in Phys. Rev. C).
- [13] J. Boguta and A.R. Bodmer, Nucl. Phys. A **292**, 413 (1977); J. Boguta and H. Stöcker, Phys. Lett. **120B**, 289 (1983).
- [14] A.R. Bodmer, Nucl. Phys. A **526**, 703 (1991).
- [15] M. M. Sharma, M. A. Nagarajan, and P. Ring, Phys. Lett. B **312**, 377 (1993).

- [16] Y. Sugahara, H. Toki and P. Ring, Theor. Phys. **92**, 803 (1994).
- [17] D. Diakonov, V. Petrov, and M. V. Polyakov, Z. Phys. A **359**, 305 (1997).
- [18] T. Nakano *et al.* [LEPS Collaboration], Phys. Rev. Lett. **91**, 012002(2003).
- [19] J. Barth *et al.* [SAPHIR Collaboration], Phys. Lett. B **572**, 127 (2003).
- [20] A. Airapetian *et al.*, Phys. Lett. B **585**, 213 (2004).
- [21] V. V. Barmin *et al.* [DIANA Collaboration], Phys. Atom. Nucl. **66**, 1715 (2003).
- [22] S. Stepanyan *et al.* [CLAS Collaboration], Phys. Rev. Lett. **91**, 252001 (2003).
- [23] V. Kubarovskiy *et al.*, Phys. Rev. Lett. **92**, 032001 (2004); Erratum-ibid. **92**, 049902 (2004).
- [24] S. Chekanov *et al.* [ZEUS Collaboration], Phys. Lett. B **591**, 7 (2004).
- [25] S. Eidelman and K. G. Hayes *et al.*, Phys. Lett. B **592**, 1 (2004).
- [26] G. A. Miller, arXiv:nucl-th/0402099.
- [27] H. C. Kim, C. H. Lee, and H. J. Lee, hep-ph/0402141.
- [28] D. Cabrera, Q.B. Li, V.K. Magas, E. Oset and M.J. Vicente Vacas, arXiv:nucl-th/0407007.
- [29] F.S. Navarra, M. Nielsen and K. Tsushima, arXiv:nucl-th/0408072.
- [30] H. Shen and H. Toki, arXiv:nucl-th/0410072.
- [31] B. D. Serot and J. D. Walecka, Adv. Nucl. Phys. **16**, 1 (1986).
- [32] P.-G. Reinhard, Rep. Prog. Phys. **52**, 439 (1989).
- [33] K. Tsushima, K. Saito, J. Haidenbauer, A.W. Thomas, Nucl. Phys. A **630**, 691 (1998).
- [34] J. D. Walecka, Ann. Phys. (N. Y.), **83**, 491 (1974).
- [35] P. A. M. Guichon, K. Saito, E. Rodionov, and A. W. Thomas, Nucl. Phys. A **601**, 349 (1996); P. A. M. Guichon, K. Saito, and A. W. Thomas, Aust. J. Phys. **50**, 115 (1996).
- [36] H. Lenske and C. Fuchs, Phys. Lett. B **345**, 355 (1995).
- [37] C. Fuchs, H. Lenske and H. H. Wolter, Phys. Rev. C **52**, 3043 (1995).
- [38] S. Typel and H. H. Wolter, Nucl. Phys. A **656**, 331 (1999).
- [39] Jürgen Schaffner, Igor N. Mishustin and Takob Bondorf, Nucl. Phys. A **625**, 325 (1997).
- [40] R. Machleidt, K. Holinde, and C. Elster, Phys. Rep. **149**, 1 (1987).
- [41] E. Shuryak and V. Thorsson, Nucl. Phys. A **536**, 739 (1992).
- [42] G.Q. Li, C.-H. Lee, and G.E. Brown, Nucl. Phys. A **625**, 372 (1997).
- [43] G.E. Brown and C.-H. Lee *et al.*, Nucl. Phys. A **567**, 937 (1994).
- [44] G.E. Brown and M. Rho, Phys. Rep. **269**, 333 (1996).
- [45] M. Karliner and H. Lipkin, arXiv:hep-ph/0307243.
- [46] M. Karliner and H. Lipkin, arXiv:hep-ph/0307343.
- [47] Felipe J. Llanes-Estrada, E. Oset and V. Mateu, Phys. Rev. C **69**, 055203(2004).
- [48] P. Bicudo and G. M. Marques, Phys. Rev. D **69**, 011503 (2004).
- [49] E. Oset, S. Sarkar *et al.*, arXiv:nucl-th/0410071.
- [50] W. Cassing and E.L. Bratkovskaya, Phys. Rep. **308**, 65 (1999).

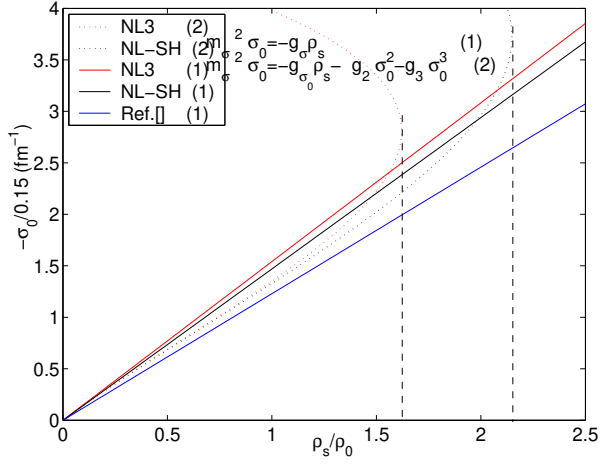


Figure 1: The scalar mean-field value as a function of the scalar density.

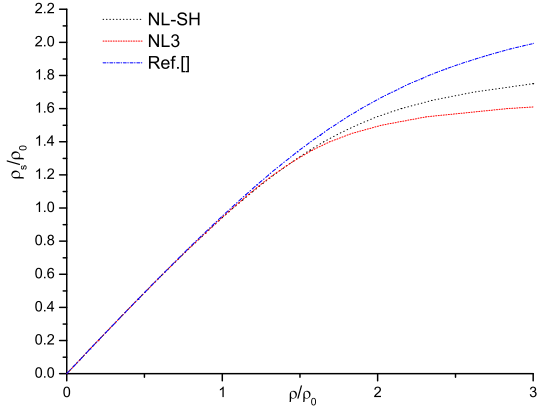


Figure 2: The scalar density as a function of the baryon density for different parameter set.

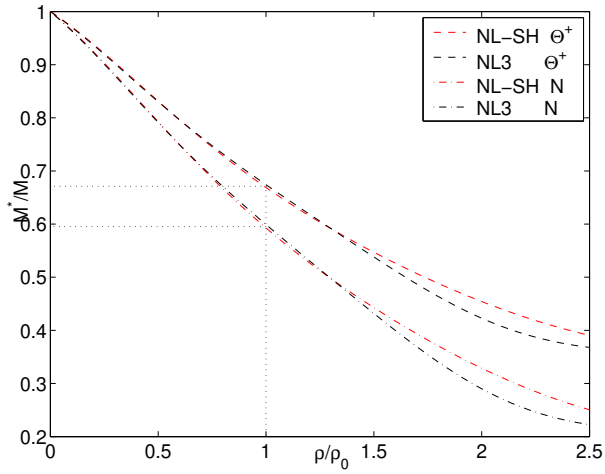


Figure 3: The ratios of effective masses of nucleon and Θ^+ in nuclear medium to those of in free space with parameter sets NL-SH and NL3.

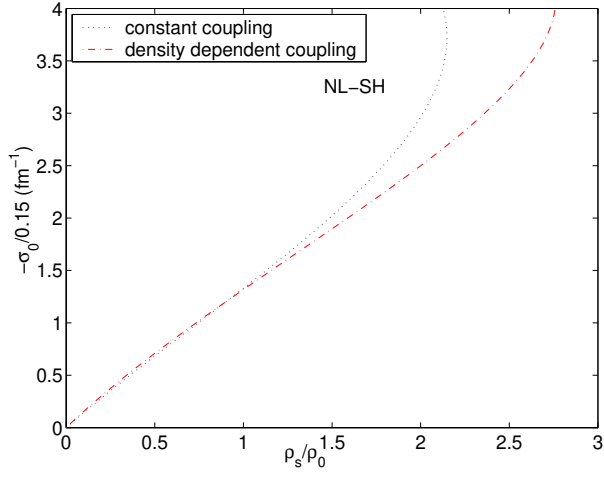


Figure 4: the scalar mean-field value as a function of the scalar density for constant scalar coupling and density dependent scalar coupling.

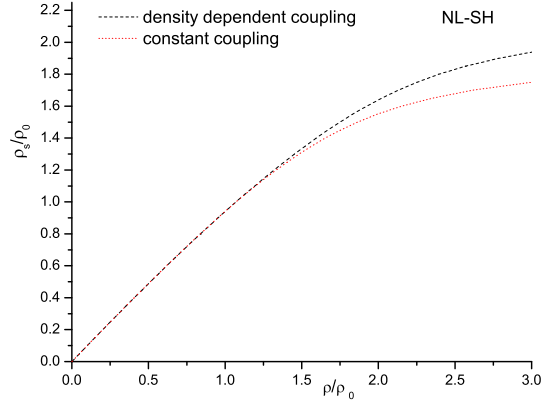


Figure 5: The scalar density as a function of the baryon density for constant scalar coupling and density dependent scalar coupling.

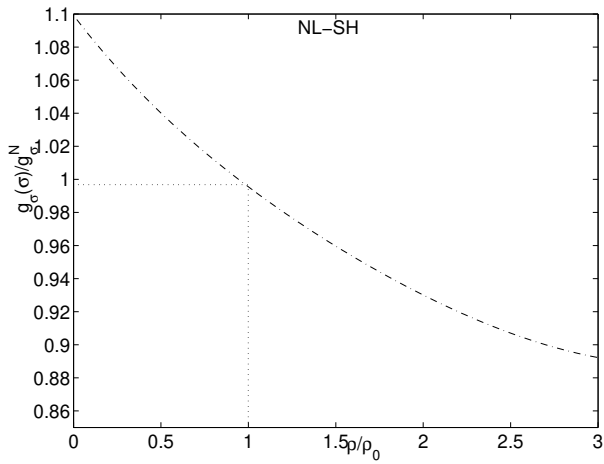


Figure 6: The density dependent scalar coupling as a function baryon density.

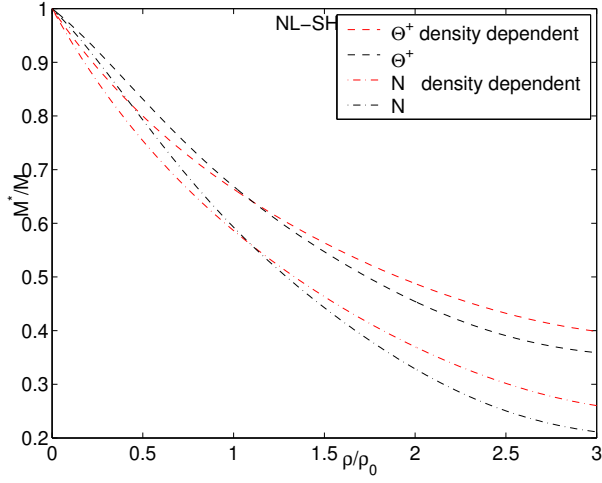


Figure 7: The ratios of effective masses of nucleon and Θ^+ in nuclear medium to those of in free space for constant scalar coupling and density dependent scalar coupling.

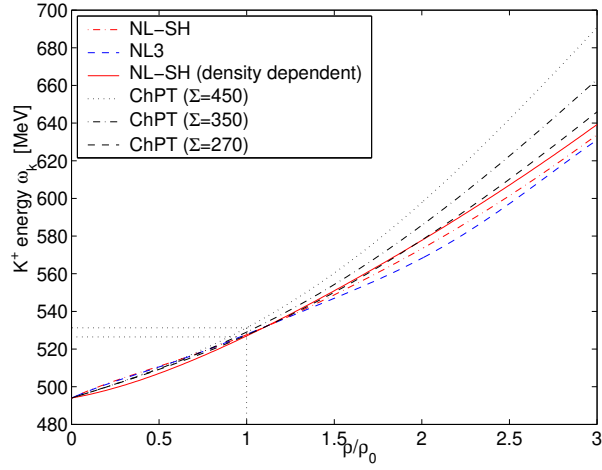


Figure 8: K^+ energy as a function baryon density for RMF model and ChPT model.

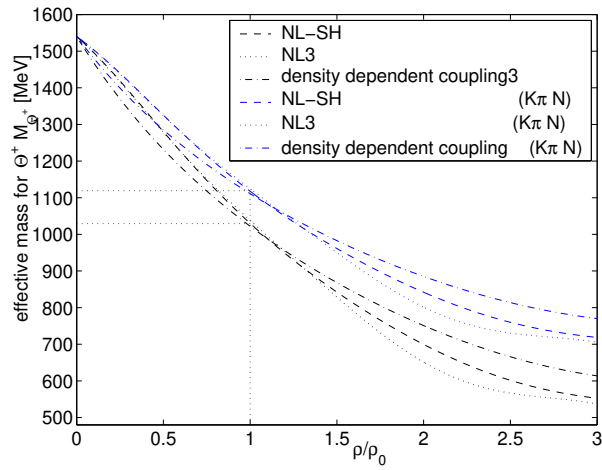


Figure 9: The effective mass for Θ^+ as non-structure particle and $K\pi N$ bound state in nuclear medium with parameter sets NL-SH, NL3 and density dependent coupling .

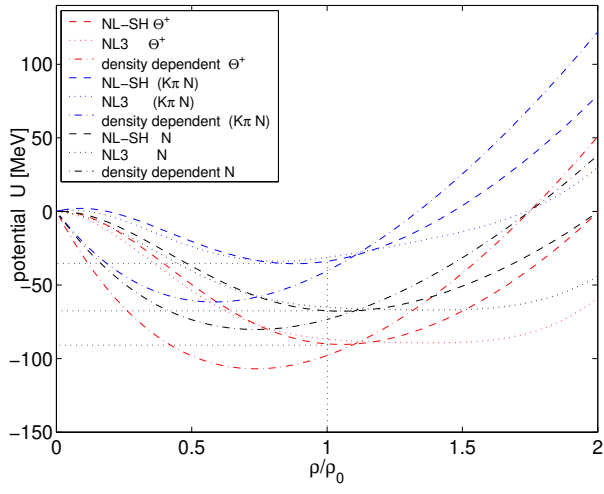


Figure 10: The potential depth of nucleon, Θ^+ as non-structure particle and $K\pi N$ bound state in nuclear medium with parameter sets NL-SH, NL3 and density dependent coupling .